JACS
JOURNAL OF THE AMERICAN CHEMICAL SOCIETY
Communication
pubs.acs.org/JACS

Addressable Carbene Anchors for Gold Surfaces

Aleksandr V. Zhukhovitskiy, Michael G. Mavros, Troy Van Voorhis, and Jeremiah A. Johnson*

Department of Chemistry, Massachusetts Institute of Technology, 77 Massachusetts Avenue, Cambridge, Massachusetts 02139, United States

Supporting Information

ABSTRACT: New strategies to access functional monolayers could augment current surface modification methods. Here we present addressable *N*-heterocyclic carbene (ANHC) anchors for gold surfaces. A suite of experimental and theoretical methods was used to characterize ANHC monolayers. We demonstrate grafting of highly fluorinated polymers from surface-bound ANHCs. This work establishes ANHCs as viable anchors for gold surfaces.

Since its discovery in 1983,[1] the chemisorption of thiols on gold surfaces has enabled countless technological advances in the fields of electronics,[2] sensing,[3] microfabrication,[4] and nanotechnology.[5] Despite this broad utility, S−Au monolayers have limitations. For example, the relatively weak S−Au bond (~45 kcal/mol)[6] can lead to monolayer desorption at moderate temperatures (~100−150 °C).[6,7] Furthermore, S−Au monolayers often have ill-defined binding geometries.[8] Finally, S−Au bonds typically have low conductance, which could limit their use in molecular electronics applications.[9]

Other anchor groups have been explored for binding to gold surfaces. Though some of these, such as alkyl[10,11] and dithiocarbamate,[9] display increased conductance or improved binding strength, there is still need for a general, synthetically versatile complement to Au−S monolayer formation.

We were drawn to *N*-heterocyclic carbenes (NHCs)[12] as a potentially useful class of reagents for binding to inorganic surfaces (Figure 1). NHCs offer a combination of exceptional

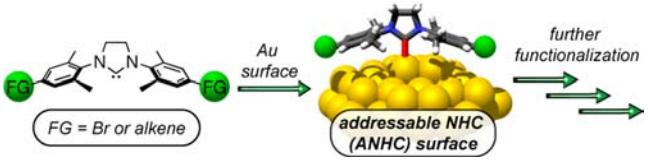

Figure 1. Functionalization of gold with ANHCs.

σ-donating and moderate π-backbonding ability,[13] which has made them ligands of choice for late transition metals like Ru(II)[14,15] and Au(I).[16] We envisioned that these same characteristics could lead to strong, partially conjugated surface bonds. Furthermore, the synthetic flexibility of NHCs could facilitate their general use for surface functionalization.

To date, one published work[17] explored the use of NHCs for coating planar gold surfaces; three reports[18−20] entertained gold nanoparticle stabilization with NHCs. While these studies are encouraging, they provide no details for such parameters as bond strength, rate of adsorption, layer density, or electronic structure. Moreover, the exclusively *N*,*N*-dialkyl NHCs described rendered the surfaces inert toward further functionalization.

To study NHC-gold surface binding and facilitate NHC monolayer functionalization, we prepared (Scheme S1) two "addressable NHCs" (ANHCs) that possess aryl bromide[21] (**1**, Figure 2A) and β-methylstyrene (**2**, Figure 2A) functional

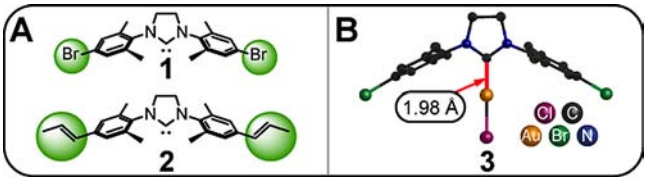

Figure 2. (A) ANHC structures. (B) Crystal structure of complex **3**.

groups. Both ANHCs form mono- and bis-Au(I) complexes (e.g., **3**, Figure 2B) upon exposure to $(Ph_3P)AuCl$ in THF (Scheme S2). The crystal structure of **3** features a C−Au bond length of 1.98 Å, which is consistent with reported values for IMes- and SIMes-Au(I) complexes (2.00 and 1.98 Å, respectively).[22] Of note, this bond length is much shorter than the Au−S bond length (2.2−2.6 Å) observed in crystal structures of thiolate-stabilized gold nanoparticles.[23]

Quartz crystal microbalance with dissipation (QCM-D) was used to study binding of **1** and commercially available IMes to gold surfaces. For all QCM-D experiments, a THF solution of free carbene was flowed over a gold-coated sensor; binding was characterized via changes in frequency (F) and dissipation (D) of the sensor. The carbene solutions were prepared as follows (see SI for details):

(a) For **1** and **2**, a THF suspension of imidazolium salt ANHC precursor (**IS1** or **IS2**, respectively, Scheme S1) was exposed to potassium hexamethyldisilazide (KHMDS, 1.0 equiv) under N_2. The resulting solution was filtered through a 0.25 μm syringe filter.

(b) For IMes, IMes was dissolved in THF under N_2. The solution was filtered through a 0.25 μm filter.

Both carbene solutions initiated a rapid frequency change upon introduction to the QCM-D sensor; saturation was approached within 15 min (Figure 3A, B). As expected for rigid monolayers,[24] the surfaces were characterized by small ratios of $\Delta D{:}\Delta F$ ($\ll 4 \times 10^{-7}$ Hz^{-1}). The areal mass density (AMD) of bound species was estimated using the Sauerbrey method.[24,25]

Received: February 26, 2013
Published: May 13, 2013

   dx.doi.org/10.1021/ja401965d | J. Am. Chem. Soc. 2013, 135, 7418−7421

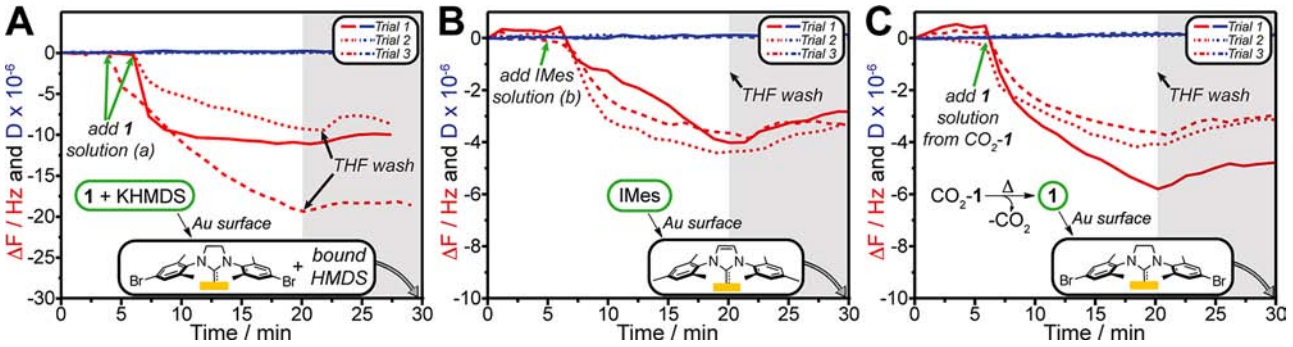

Figure 3. QCM-D traces for carbene solutions. (A) Solution (a): ANHC **1** generated via exposure of **IS1** to KHMDS in THF. (B) Solution (b): Commercially available NHC IMes in THF. (C) THF solution of ANHC **1** generated via decarboxylation of CO_2-**1** (no KHMDS present). The measured areal mass densities (AMDs) for each sample are 210 ± 80, 56 ± 6, and 63 ± 14 ng/cm^2, respectively.

Average AMD values for **1** and IMes taken from three measurements were 210 ± 80 and 56 ± 6 ng/cm^2, respectively.

Control experiments with HMDS amine or amide in the absence of carbene showed little binding of the former, but significant binding of the latter (Figure S1). Thus, we hypothesized that binding of residual HMDS amide led to the larger AMD, and increased deviation, for **1** compared to IMes.

To test this hypothesis, a solution of **1** in THF was prepared via thermal decarboxylation of an independently synthesized CO_2-**1** adduct (Scheme S3). The average AMD value for this solution of **1** without HMDS was 63 ± 14 ng/cm^2 (Figure 3C), which agrees well with the value for IMes.

Based on the dimensions of **1** obtained via crystallography (Figure 2B), we estimate the maximum possible AMD for a monolayer of **1** on a perfectly flat surface to be 85 ng/cm^2. This limit would be higher for a rough surface. Given the steric bulk of **1** and IMes, the measured AMDs (~63 and ~56 ng/cm^2, respectively) are reasonable.

Monolayers of **1** and IMes prepared via immersion of gold-coated silicon wafers in solution (a) or (b), respectively, were characterized by narrow-scan X-ray photoelectron spectroscopy (XPS). The spectra were normalized to the transmission-corrected area of the carbon peaks (Figure 4A). The surface exposed to **1** showed a significant Br signal (Figure 4B). The measured Br/N ratio of 0.16:1 corresponds to a mixed monolayer with 21% **1** and 79% HMDS by mass (Table S1).

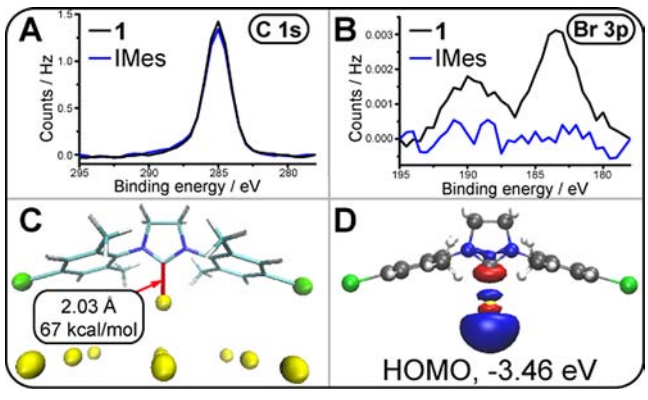

Figure 4. (A) C 1s and (B) Br 3p regions of the XPS spectra for **1** and IMes bound to planar gold surfaces. (C) DFT model of **1** bound to a gold surface. (D) HOMO of the **1**-Au(0) complex.

Surfaces treated with IMes showed no detectable Br (Figure 4B).

In order to gain further insight into the nature of the NHC-Au surface interaction, density functional theory (DFT) was used to model the binding of **1** to a charge-neutral gold adatom above a fixed gold lattice. The calculated structure (Figure 4C) possesses a C−Au bond length of 2.03 Å, which agrees well with that of the crystal structure for **3**. Furthermore, the calculated homolytic Au−C bond dissociation energy (BDE) was found to be 67 kcal/mol, which is more than 20 kcal/mol larger than a typical Au−S bond. Calculations performed using either a single gold atom or gold clusters produced similar **1**-Au σ-bonding orbitals, which suggests that the bonding is highly localized to a single gold atom.

We next studied the electronic structure of the **1**-Au bond via DFT using the B3LYP functional; the basis set was LANL2DZ + effective core potential for gold, and 6-31g* for all other atoms. For clarity, we present results (Figures 4D and S2) from the simplest (one gold atom) model. The electron density in the HOMO (Figure 4D) is delocalized over the gold atom *and* the carbene carbon; this delocalization extends to the nitrogen atoms in the HOMO. These results suggest that ANHCs could form conductive surface linkages.

Next we sought to demonstrate chemical modification of an ANHC-gold surface. Attempts to perform various metal-catalyzed cross-coupling reactions on **1**-Au surfaces were met with difficulty due to nonspecific adsorption. Thus, we focused on modification of the olefins of **2**-Au monolayers. We envisioned that treatment of **2**-Au surfaces with third-generation Grubbs catalyst[26] (***Ru***, Figure 5A) would generate surface-bound initiators for ring-opening metathesis polymerization (ROMP).[27,28]

A series of model experiments using an isolated bis-**2**-Au complex demonstrated that cross-metathesis between ***Ru*** and **2** was efficient in solution (Figures S3−S5, Table S2). Encouraged by these results, we performed the sequence of reactions depicted in Figure 5A on a gold-coated QCM-D sensor; relevant steps are labeled ***i***−***vi***. First, exposure of the sensor to a 0.21 mM solution of **2** (prepared via method (a)) for 15 min (region ***i***) followed by a wash with fresh THF (region ***ii***) resulted in an AMD of 230 ng/cm^2. If we assume that **2** binds to the surface with equal affinity to IMes, then ~61 ng/cm^2 of this AMD value corresponds to **2**.

The surface was then exposed to a 5.80 mM solution of ***Ru*** in THF for 5 h (region ***iii***). Another THF wash was performed (region ***iv***). At this stage, the surface consisted of putative Ru-benzylidene complexes bound via the **2**-Au linkage (***Ru***-**2**-**Au**

dx.doi.org/10.1021/ja401965d | J. Am. Chem. Soc. 2013, 135, 7418−7421

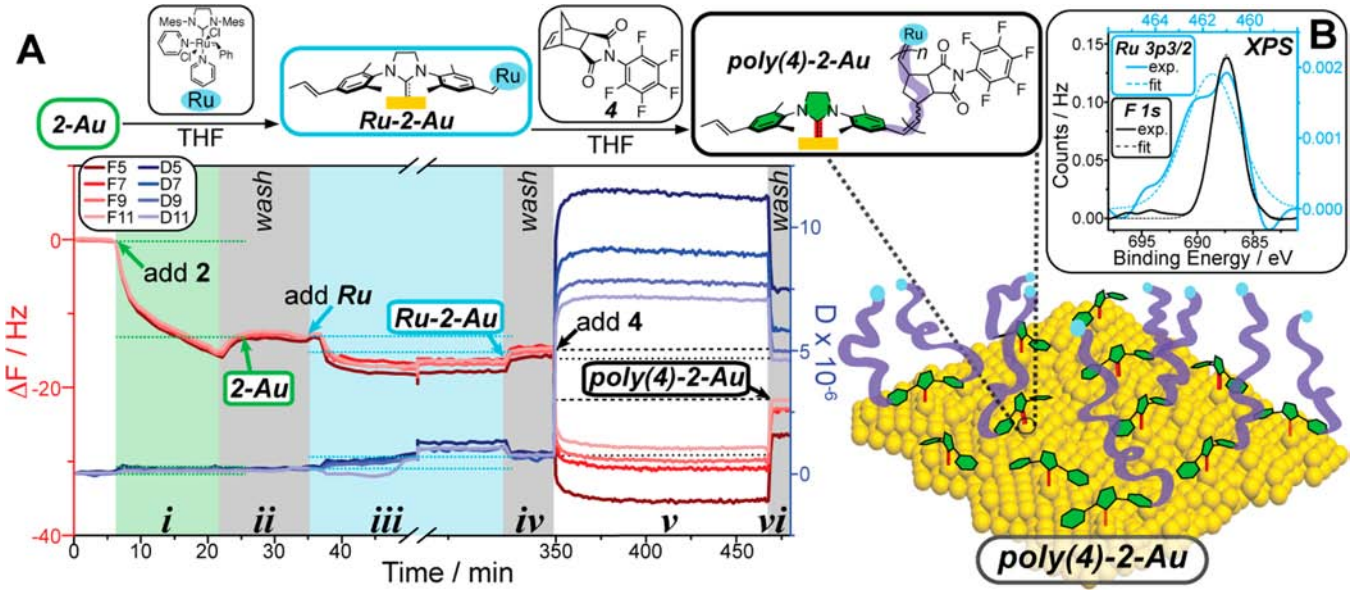

Figure 5. (A) Scheme for ROMP from **2-Au** surfaces and QCM-D data for the surface functionalization process. Red and blue curves correspond to various frequency (*Fj*, inset legend) and dissipation (*Dj*, inset legend) overtones, respectively. (B) F 1s and Ru 3p3/2 regions of the XPS spectrum of **poly(4)-2-Au**.

surface). The **2-Au** to ***Ru*-2-Au** process coincided with a ~2.6 Hz frequency change, and a significant change in dissipation (from ~0.2 × 10^{-6} to ~0.7 × 10^{-6}). The Voigt model[29,30] was used to calculate an AMD of 60 ng/cm^2 of bound ***Ru*** (see SI for details). This AMD combined with the estimated AMD of **2** (61 ng/cm^2) corresponds to ~39% olefin conversion, which is consistent with the percentage of cross metathesis observed in solution studies (Figure S5).

Subsequent exposure of the surface to pentafluorophenyl *exo*-norbornene derivative **4** (0.121 M in THF) for 2 h (region ***v***) resulted in drastically altered frequency and dissipation values along with an observed dispersion in $(1/j)\Delta f$ for different overtones j (Figure 5A). These results are consistent with growth of a soft polymer brush from the surface (**poly(4)-2-Au**).[24] The ΔAMD from polymerization was 1520 ng/cm^2, which, if polymer solvation is neglected, translates to an average degree of polymerization (DP) of 35.

No polymerization was observed when the same sequence of events was carried out using **1** rather than **2** (Figure S6A), which confirms the role of the olefinic groups of **2**. Finally, exposure of a **2**-Au surface to monomer **4** in the absence of ***Ru*** gave no change in dissipation and a ΔAMD of ~53 ng/cm^2 from nonspecific adsorption (Figure S7A); no polymerization occurred.

XPS analysis was performed on the same surfaces used for QCM-D experiments (Figures 5B, S6B, and S7B; Table S1). As expected, the **poly(4)-2-Au** surface exhibited high fluorine content along with Ru (Figure 5B). Control samples with **1** or no ***Ru*** showed much lower fluorine signal from adsorbed **4**. The Ru/F ratio for **poly(4)-2-Au** (see footnote for Table S1) was used to calculate an average brush DP of 18 (assuming one Ru atom per polymer chain and five F atoms per polymer repeat unit). The difference in DP compared to QCM-D is likely due to polymer solvation.[31]

Tapping-mode atomic force microscopy (AFM) of these surfaces revealed a marked difference in roughness. **Poly(4)-2-Au** had a roughness (RMS) of 5.6 nm (Figure 6A). In contrast, the roughness of control sensors was 1.4 nm (no ***Ru***, Figure 6B) and 2.0 nm (**1**-Au monolayer, Figure S8), which matches that reported for bare sensors (3 nm).[32] The elongated features present only in the AFM image of **poly(4)-2-Au** (Figure 6A) resemble those reported for other poly-norbornene grafted surfaces.[27]

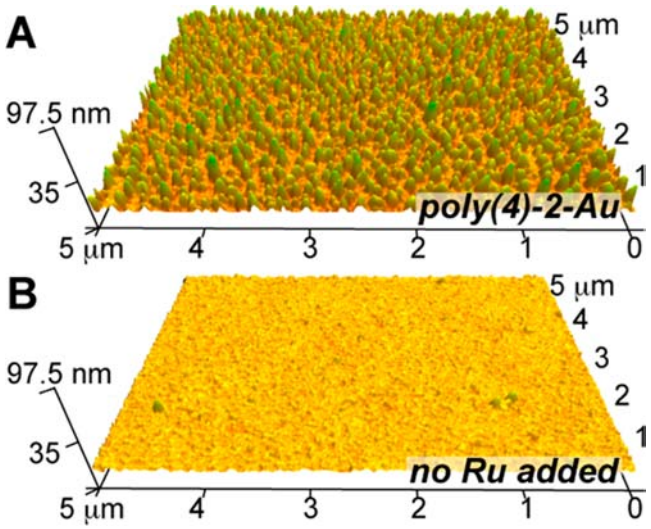

Figure 6. AFM characterization of (A) **poly(4)-2-Au** surface and (B) control surface with no ***Ru*** catalyst added.

In this report we have described the first examples of gold surface functionalization with addressable *N*-heterocyclic carbenes. We describe details of the ANHC-surface binding interaction and demonstrate the growth of novel polymer brushes from robust ANHC monolayers. We expect that these results will spark interest in the use of ANHCs and other stable carbenes as general surface anchors.

■ ASSOCIATED CONTENT

Supporting Information

Supplemental figures, schemes, tables, calculations, specifications of DFT analysis, detailed synthetic procedures, and

spectral and crystallographic data. This material is available free of charge via the Internet at http://pubs.acs.org.

AUTHOR INFORMATION

Corresponding Author

jaj2109@mit.edu

Notes

The authors declare no competing financial interest.

ACKNOWLEDGMENTS

We thank the Deshpande Center for Technological Innovation, the MIT Lincoln Laboratories, and the DoD NDSEG program for support of this work. This work made use of the MRSEC Shared Experimental Facilities at MIT (NSF, DMR-08-19762) and the MIT X-Ray Facility (NSF, CHE-0946721). We thank J. Im, R. Faust, and L. Ren for help with QCM-D experiments, P. Müller for X-ray crystallography, and J. E. Whitten and Y. Wang for supplemental XPS characterization.

REFERENCES

(1) Nuzzo, R. G.; Allara, D. L. *J. Am. Chem. Soc.* **1983**, *105*, 4481.
(2) DiBenedetto, S. A.; Facchetti, A.; Ratner, M. A.; Marks, T. J. *Adv. Mater.* **2009**, *21*, 1407.
(3) Ranieri, A.; Monari, S.; Sola, M.; Borsari, M.; Battistuzzi, G.; Ringhieri, P.; Nastri, F.; Pavone, V.; Lombardi, A. *Langmuir* **2010**, *26*, 17831.
(4) Koh, S. *Nanoscale Res. Lett.* **2007**, *2*, 519.
(5) Love, J. C.; Estroff, L. A.; Kriebel, J. K.; Nuzzo, R. G.; Whitesides, G. M. *Chem. Rev.* **2005**, *105*, 1103.
(6) Nuzzo, R. G.; Zegarski, B. R.; Dubois, L. H. *J. Am. Chem. Soc.* **1987**, *109*, 733.
(7) Cometto, F. P.; Patrito, E. M.; Paredes Olivera, P.; Zampieri, G.; Ascolani, H. *Langmuir* **2012**, *28*, 13624.
(8) Pensa, E.; Cortés, E.; Corthey, G.; Carro, P.; Vericat, C.; Fonticelli, M. H.; Benítez, G.; Rubert, A. A.; Salvarezza, R. C. *Acc. Chem. Res.* **2012**, *45*, 1183.
(9) von Wrochem, F.; Gao, D.; Scholz, F.; Nothofer, H.-G.; Nelles, G.; Wessels, J. M. *Nat. Nanotechnol.* **2010**, *5*, 618.
(10) Cheng, Z. L.; Skouta, R.; Vazquez, H.; Widawsky, J. R.; Schneebeli, S.; Chen, W.; Hybertsen, M. S.; Breslow, R.; Venkataraman, L. *Nat. Nanotechnol.* **2011**, *6*, 353.
(11) Chen, W.; Widawsky, J. R.; Vázquez, H.; Schneebeli, S. T.; Hybertsen, M. S.; Breslow, R.; Venkataraman, L. *J. Am. Chem. Soc.* **2011**, *133*, 17160.
(12) Kirmse, W. *Angew. Chem., Int. Ed.* **2010**, *49*, 8798.
(13) Jacobsen, H.; Correa, A.; Poater, A.; Costabile, C.; Cavallo, L. *Coord. Chem. Rev.* **2009**, *253*, 687.
(14) Huang, J.; Stevens, E. D.; Nolan, S. P.; Petersen, J. *J. Am. Chem. Soc.* **1999**, *121*, 2674.
(15) Scholl, M.; Trnka, T. M.; Morgan, J. P.; Grubbs, R. H. *Tetrahedron Lett.* **1999**, *40*, 2247.
(16) Nolan, S. P. *Acc. Chem. Res.* **2010**, *44*, 91.
(17) Weidner, T.; Baio, J. E.; Mundstock, A.; Grosse, C.; Karthaeuser, S.; Bruhn, C.; Siemeling, U. *Aust. J. Chem.* **2011**, *64*, 1177.
(18) Serpell, C. J.; Cookson, J.; Thompson, A. L.; Brown, C. M.; Beer, P. D. *Dalton Trans.* **2013**, *42*, 1385.
(19) Vignolle, J.; Tilley, T. D. *Chem. Commun.* **2009**, 7230.
(20) Hurst, E. C.; Wilson, K.; Fairlamb, I. J. S.; Chechik, V. *New J. Chem.* **2009**, *33*, 1837.
(21) Süßner, M.; Plenio, H. *Chem. Commun.* **2005**, 5417.
(22) de Frémont, P.; Scott, N. M.; Stevens, E. D.; Nolan, S. P. *Organometallics* **2005**, *24*, 2411.
(23) Jadzinsky, P. D.; Calero, G.; Ackerson, C. J.; Bushnell, D. A.; Kornberg, R. D. *Science* **2007**, *318*, 430.
(24) Reviakine, I.; Johannsmann, D.; Richter, R. P. *Anal. Chem.* **2011**, *83*, 8838.
(25) Sauerbrey, G. *Z. Phys.* **1959**, *155*, 206.
(26) Love, J. A.; Morgan, J. P.; Trnka, T. M.; Grubbs, R. H. *Angew. Chem., Int. Ed.* **2002**, *41*, 4035.
(27) Kong, B.; Lee, J. K.; Choi, I. S. *Langmuir* **2007**, *23*, 6761.
(28) Weck, M.; Jackiw, J. J.; Rossi, R. R.; Weiss, P. S.; Grubbs, R. H. *J. Am. Chem. Soc.* **1999**, *121*, 4088.
(29) Johannsmann, D. *Phys. Chem. Chem. Phys.* **2008**, *10*, 4516.
(30) Voinova, M. V.; Rodahl, M.; Jonson, M.; Kasemo, B. *Phys. Scr.* **1999**, *59*, 391.
(31) Müller, M. T.; Yan, X.; Lee, S.; Perry, S. S.; Spencer, N. D. *Macromolecules* **2005**, *38*, 5706.
(32) Reported by QSense on www.q-sense.com/sensors-and-coatings-1.